Cavity Enhanced Spectroscopy of High-Temperature H₂O in the Near-Infrared Using a Supercontinuum Light Source

ROSALYNNE S. WATT, TONI LAURILA, CLEMENS F. KAMINSKI,* and JOHAN HULT

Department of Chemical Engineering and Biotechnology, University of Cambridge, Pembroke Street, CB2 3RA Cambridge, UK (R.S.W., T.L., C.F.K., J.H.); and SAOT School of Advanced Optical Technologies, Max Planck Institute for the Science of Light, Guenther-Scharowsky-Strasse 1, D-91058 Erlangen, Germany (C.F.K.)

In this paper we demonstrate how broadband cavity enhanced absorption spectroscopy (CEAS) with supercontinuum (SC) radiation in the near-infrared spectral range can be used as a sensitive, multiplexed, and simple tool to probe gas-phase species in high-temperature environments. Near-infrared SC radiation is generated by pumping a standard single-mode fiber with a picosecond fiber laser. Standard low reflectivity mirrors are used for the cavity and an optical spectrum analyzer is used for the detection of gas-phase species in combustion. The method is demonstrated by measuring flame generated H₂O in the 1500 to 1550 nm region and room-temperature CO₂ between 1520 nm and 1660 nm. The broadband nature of the technique permits hundreds of rotational features to be recorded, giving good potential to unravel complex, convoluted spectra. We discuss practical issues concerning the implementation of the technique and present a straightforward method for calibration of the CEAS system via a cavity ringdown measurement. Despite the large spectral variation of SC radiation from pulse to pulse, it is shown that SC sources can offer good stability for CEAS where a large number of SC pulses are typically averaged.

Index Headings: Supercontinuum; Cavity enhanced spectroscopy; Cavity ringdown spectroscopy.

INTRODUCTION

Supercontinuum (SC) radiation[1,2] has enhanced a range of technologies in the life and chemical sciences, including microscopy[3] and optical measurement techniques,[4] and is increasingly finding its way into chemical species sensing.[3,5–9] Recently, SC radiation has been used for extremely rapid broadband gas sensing[5] and for high sensitivity cavity enhanced absorption spectroscopy (CEAS) over wide spectral regions in the visible range.[7,8] In CEAS an optical cavity is employed in order to increase the sample absorption path length and thus to achieve the high sensitivity required for trace gas detection. Experimentally, CEAS entails irradiation of a sample gas inside an optical cavity with light and measurement of the steady-state intensity transmitted through the cavity. The transmitted intensity depends on the attenuation of the light trapped within the cavity, part of which is caused by absorption by the sample to be analyzed.

Measurements over wide spectral regions have been demonstrated using a variety of broadband light sources, such as incoherent light emitting diodes (LEDs),[10] discharge lamps,[11] or frequency comb sources.[12] In comparison to LEDs and lamp sources, the coherent sources offer higher spectral brightness, permitting more rapid measurements to be performed. In the frequency comb approach[12] the modes of the laser source are actively locked to the mode structure of the cavity to ensure resonant light coupling into the cavity, and this adds significant complexity to the experimental setup. In contrast, we here use the optical cavity in a non-confocal alignment, which results in a quasi-continuous cavity mode structure.[13] The cavity is set up on an optical table using standard kinematic mirror mounts, and no special efforts are made to prevent small scale mechanical movements caused by structural vibrations and density fluctuations in the sample gas. This is deliberate and works to our advantage as any residual mode structure remaining in the cavity is quickly averaged out. The resulting quasi-continuous mode structure of the low-finesse cavity combined with the dense mode structure of the supercontinuum source (the latter is not frequency stabilized and has a mode spacing of only 0.3 MHz) ensures that on average the entire broadband emission from the SC source is transmitted through the cavity without any requirement for active longitudinal cavity mode matching, which is in contrast to the reported frequency comb approach.[12] As a result, the experimental setup is greatly simplified and robust. A disadvantage is that the overall efficiency with which light is coupled into the optical cavity is reduced, but the high spectral brightness of the SC source compensates for this problem. In the visible spectral range we have previously demonstrated ultra-sensitive CEAS measurements with this approach in signal integration times of only 2 s or less,[7] at detection limits that compare favorably with competing techniques. In the present case the light throughput is so large (because of the high transmission of the cavity) that sufficient signal-to-noise ratios are already obtained when a standard optical spectrum analyzer is used to disperse and record the resulting signals.

Some of the CEAS work using broadband light sources has been performed in the near-infrared (NIR) spectral region.[12,14–16] In combustion studies NIR sources are of particular interest as many vibrational overtones of species of interest lie in this region, allowing concentration and temperature measurements.[5,18] In this work NIR SC radiation, generated by pumping a conventional single-mode fiber with a picosecond fiber laser,[19] is employed for SC-based CEAS of flames for the first time. The demonstration is performed in a laminar flat flame burner by measuring hot water vapor in the 1500–1550 nm spectral range. This spectral region was selected in order to avoid the interference from the much stronger room-temperature lines appearing around 1400 nm. Cavity mirrors of modest reflectivity (~98%) were used in order to achieve sufficient throughput for detection by a standard optical spectrum analyzer (OSA), while still allowing a suitable signal enhancement to detect the weak high-temperature absorption lines that would be difficult to observe in a direct absorption measurement. Previous CEAS studies in flames, e.g., of H₂O and OH lines,[20–22] have all employed narrow-band laser sources, such as laser diodes. The SC
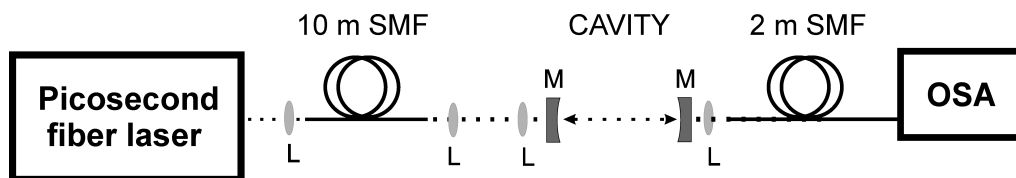
FIG. 1. Experimental setup for broadband NIR CEAS (L = lens, SMF = single mode fiber, M = cavity mirror, and OSA = optical spectrum analyzer).

radiation allows access to a broader spectral region, providing more spectroscopic information on the target molecules.

In order to obtain quantitative concentration measurements, CEAS requires an independent calibration of the mirror reflectivity. A number of techniques can be used for calibration: a reference measurement using a broadband absorber at known concentration,[7] a direct measurement of the cavity life-time using cavity ringdown spectroscopy (CRDS),[8,23] or detection of the cavity-induced phase shift.[24] Recently, broadband CRDS has been demonstrated by using filament generated supercontinuum light.[25,26] In this work the low-finesse cavity allows the reflectivity to be measured by directly recording ringdown signals in a relatively narrow spectral band using a fast photodiode as detector. In addition, near-infrared absorption bands of room-temperature CO_2 were used to independently calibrate the setup.

SPECTROMETER SETUP AND OPERATION

The experimental configuration employed for broadband CEAS is depicted in Fig. 1. Near-infrared SC radiation was generated by launching 5 ps laser pulses, centered around 1060 nm, into 10 meters of conventional single-mode fiber (Corning SMF28).[19] The pump laser was a ytterbium fiber laser (Fianium, FemtoPower-1060) featuring a variable repetition rate. Here a repetition rate of 331 kHz was employed, ensuring pulse energies high enough for efficient NIR SC generation in the single-mode fiber (SMF). An aspheric lens ($f = 6$ mm) was
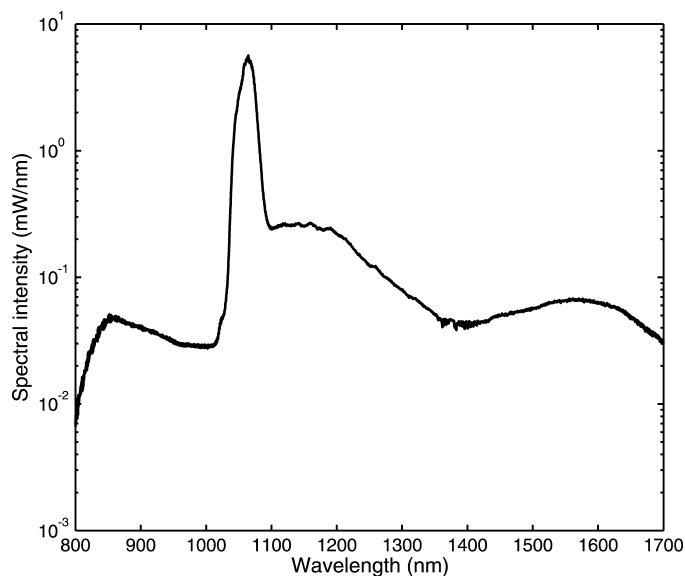

FIG. 2. Spectral profile of the NIR supercontinuum radiation spanning from 800 to 1700 nm. The SC was generated in a 10 m long conventional single-mode fiber. The spectrum was acquired with the OSA at a resolution of 2 nm. The fine scale structure visible around 1400 nm is due to absorption by ambient water vapor present inside the optical spectrum analyzer.

used for coupling light into the SMF, with a coupling efficiency of around 33%, resulting in broadband radiation spanning from 800 nm to 1700 nm. The spectral profile of the SC radiation is displayed in Fig. 2. The SC radiation exiting the SMF was collimated into a beam having a diameter of about 4 mm. The beam was then slightly focused (using an $f = 500$ mm lens) into the cavity. Two plano-concave mirrors (Comar MX 241, about 98% nominal reflectivity from 1500 nm to 1600 nm, 2 m radius of curvature) formed the optical cavity. The mirrors were separated by 1.17 m and the transmitted radiation was coupled into a 2 m long SMF and recorded using an optical spectrum analyzer (OSA, Yokogawa AQ6317Q).

The CEAS experiments were performed by measuring the steady-state intensity, I, transmitted by the optical cavity in the presence of an absorbing sample. The experimental absorbance is then calculated:

$$A_{\text{CEAS,EXP}} = \log_{10}(I_0/I) \tag{1}$$

where I_0 represents the intensity transmitted by the empty nitrogen-flushed cavity. For comparison to a theoretical spectrum the corresponding theoretical absorbance was calculated using:

$$A_{\text{CEAS,THEORY}} = -\log_{10}(T_{\text{THEORY}} \otimes \psi) \tag{2}$$

where ψ is the instrument function, $\otimes$ denotes a convolution operation, and T_{THEORY} is the theoretical transmission through the cavity assuming small cavity losses per pass and high mirror reflectivity:

$$T_{\text{THEORY}} = \frac{1}{\left(A_{\text{SP,THEORY}}/|\log_{10}[R(\lambda)]|\right) + 1} \tag{3}$$

where $A_{\text{SP,THEORY}}$ is the single-pass absorbance in the cavity, calculated using theoretical line parameters, and $R(\lambda)$ is the mirror reflectivity. This treatment of the theoretical spectrum employs the general expression for the light transmitted by the cavity by Triki et al.[27] and through the convolution also accounts for the finite spectral resolution of the instrument.[28] This is a necessary procedure in the present case when the single-pass absorbance, $A_{\text{SP,THEORY}}$, is comparable to the mirror losses, and the spectral features are under-resolved by the detection system. Light at wavelengths on-resonance with the absorption line, which has a short ringdown time, is then probed in the same spectral bin as light at wavelengths in the spectral wings, which has longer ringdown times, and consequently higher steady-state intensity inside the cavity is observed than expected.

For quantitative CEAS measurements the wavelength-resolved reflectivity of the cavity mirrors must be determined. Two techniques have been used for this purpose; a direct measurement of cavity ringdown times and a calibration with a
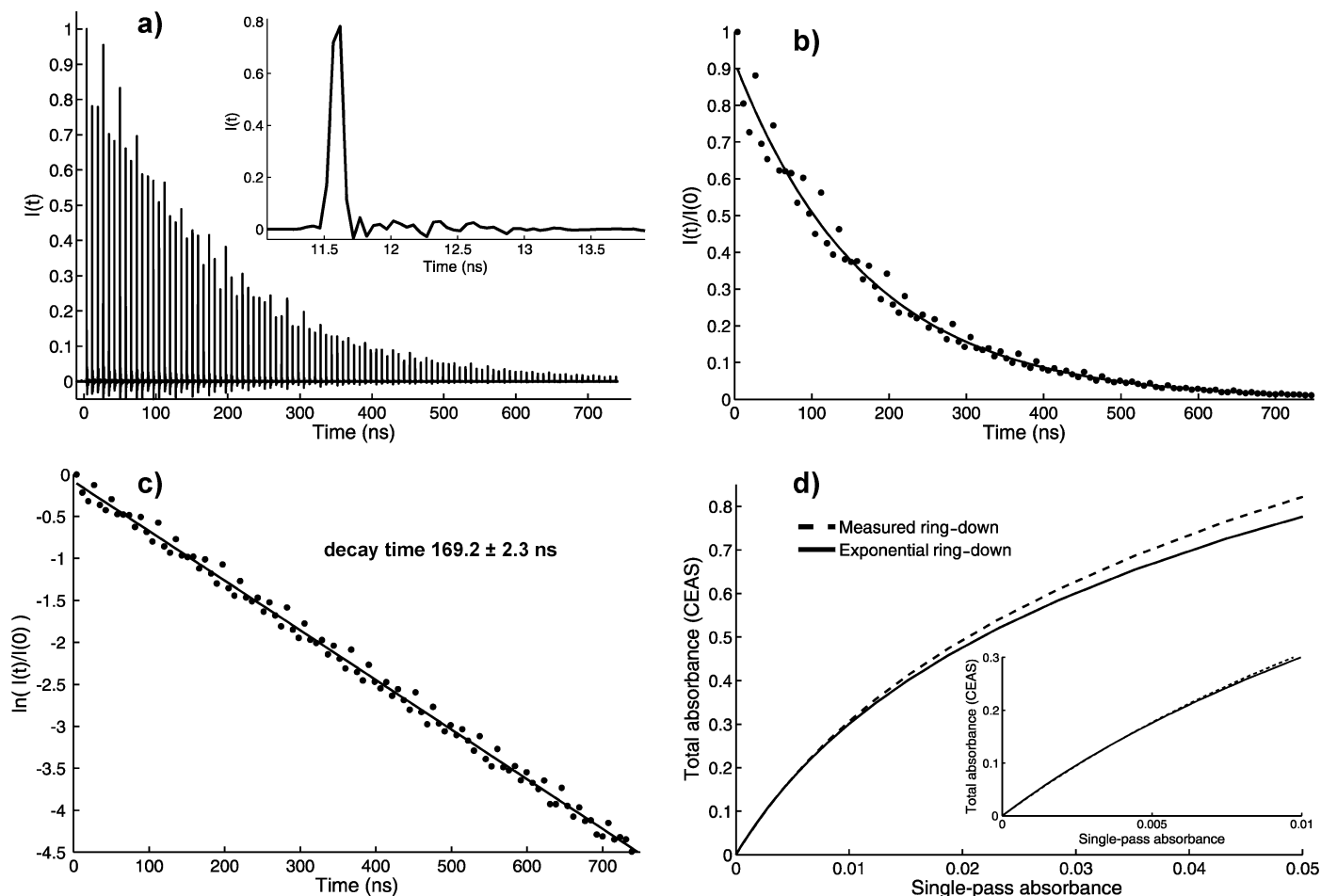
FIG. 3. (a) Bounce-by-bounce ringdown pulse profile of the 1.17 m long cavity. The inset shows an individual transmitted laser pulse. (b) Corresponding areas of individual ringdown pulses (dots) and exponential fit (solid line). (c) The pulse areas plotted on a logarithmic scale. (d) Predicted total observed absorbance versus single-pass absorbance for the measured ringdown (dashed line) and the single exponential fit (solid line).

reference sample. Both techniques are described in the following section.

CALIBRATION

Cavity Ringdown Calibration. The use of a supercontinuum source with a sub-nanosecond pulse length and a suitably fast detection system allows a direct *bounce-by-bounce* measurement of the light pulses transmitted through the empty cavity and, therefore, the determination of the effective mirror reflectivity R from the decaying envelope of the ringdown pulse train.[29] For the cavity ringdown calibration the broadband emission of the SC source was filtered using an interference filter centered at 1550 nm (Thorlabs FL1550-12, $\Delta\lambda_{FWHM} = 12$ nm). Ringdown traces were recorded by a fiber-coupled 8 GHz photodiode (Thorlabs, PDA8GS), the output of which was digitized by an 8 GHz real-time oscilloscope (Tektronix, TDS6804B). Figure 3a shows the ringdown pulse train from the cavity averaging 1000 laser shots on the oscilloscope. The ringdown profile is largely exponential, with a small high-frequency modulation. This small modulation is thought to be due to mode beating of higher order transverse modes.[28] For the 1.17 m long cavity with mirrors having 2 m radius of curvature, the longitudinal cavity mode spacing ($\Delta q = 1$) is 128 MHz and the transverse mode spacing [$\Delta(n + m) = 1$] is 47 MHz,[30] where longitudinal cavity modes are denoted by

the index q and the transverse modes by the indices n and m. The high-frequency oscillation in Fig. 3a is characterized by a period of about three cavity round-trip times or 23 ns. This corresponds to the theoretically predicted 21 ns caused by the transverse modes. However, in a non-stabilized optical cavity, mechanical instabilities and density fluctuations of the sample gas and ambient air tend to average out such mode effects.[31] Therefore, the observed mode beating is weak and the overall decay is reasonably close to a single exponential. In Fig. 3b the area under each of the transmitted pulses is plotted, whereas in Fig. 3c the same data is plotted on a logarithmic scale. It appears to be a single exponential, featuring the high-frequency modulation discussed above. The solid line is a fit of a first-order polynomial to the logarithm of the experimental data (the exponential decay curve determined from this fit is also shown as a solid line in Fig. 3b. From the fit a decay time of 169.2 ± 2.3 ns (95% confidence interval) is determined, which corresponds to an effective reflectivity $R = 97.70 \pm 0.03\%$ at 1550 nm for the present cavity.

It is worth noting that if the ringdown pulse train can be directly measured, as is the case here, even cavities featuring non-exponential or multi-exponential ringdown times can be employed for quantitative CEAS measurements. The procedure in those situations would be as follows: The experimentally measured ringdown curve is multiplied with a series of pure
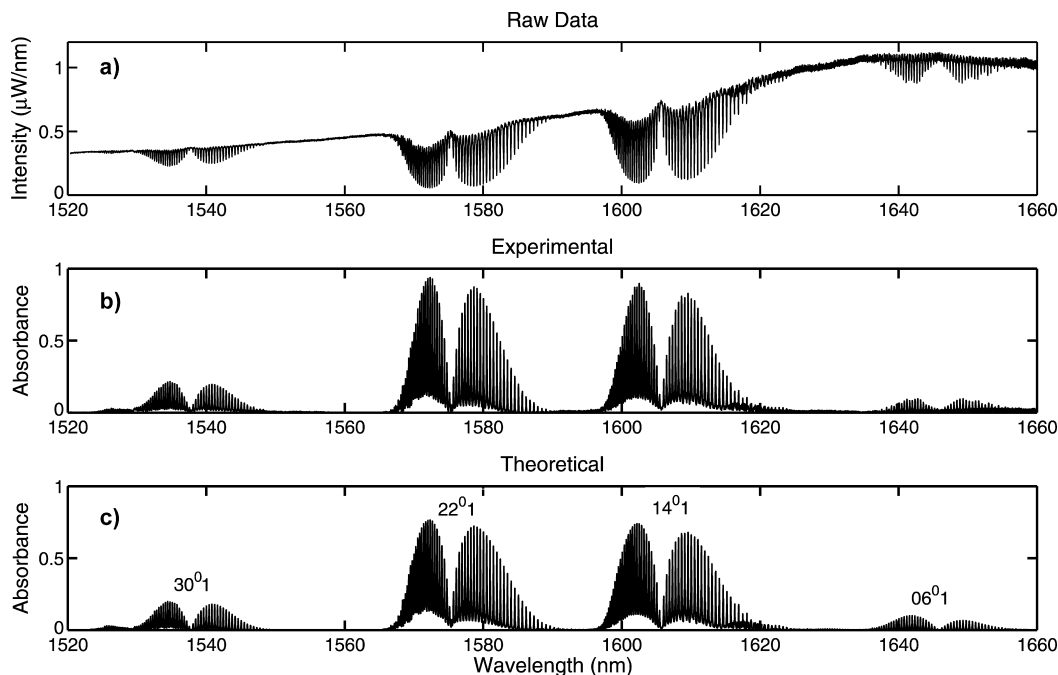
FIG. 4. (a) Measured cavity throughput when filled with 100% CO_2. (b) Corresponding CO_2 absorption spectra spanning from 1520 to 1660 nm. (c) Theoretical spectrum calculated using the line parameters from the HITRAN database at experimental conditions ($L = 1.17$ m, R varying from 0.974 at 1540 nm to 0.937 at 1640 nm, $T = 297$ K, $p = 1001$ mbar, $X_{CO2} = 1.0$). Band designations correspond to vibrational quantum numbers v_1, v_2^1, and v_3 of the excited vibrational states.[33] Above 1600 nm the response of the OSA starts to drop and the noise of the baseline increases.

exponential decays, corresponding to a range of single-pass absorbances, the results of which represent the ringdown signals out of the cavity.[27,32] From this, the corresponding CEAS signals, I, are calculated for varying single-pass absorbance by integrating the resulting ringdown curves. The CEAS reference signal, I_0, is calculated by integrating the ringdown curve from the empty cavity (i.e., the experimentally measured ringdown without absorber). From these two signals the total predicted absorbance, $\log_{10}(I_0/I)$, observed through the cavity can be calculated. This total absorbance is plotted against single-pass absorbance in Fig. 3d for both the measured ringdown curve (dashed line) and the fitted purely exponential ringdown curve (solid line). For low, here below 0.01, single-pass absorbance the two curves agree to within 2%, see inset of Fig. 3d. At larger single-pass absorbance values the curves begin to deviate; for example at a single-pass absorbance of 0.05 the difference is 6%. This is understandable as for strong absorbers most of the light injected into the cavity is absorbed quite early on within the ringdown time interval, $t < 100$ ns in Fig. 3a, which is the region of the curve where the largest peak-to-peak modulations are found. For weak absorption this is not the case, and there will be a significant fraction of photons left in the cavity for the entire duration of the ringdown time, and thus absorption takes place throughout the ringdown interval, which averages out the effects of the modulations effectively. In principle, highly modulated or multi-exponential ringdown cavities could be used for quantitative CEAS measurements, provided information on the ringdown pulse train is available. For the work presented here, however, we restrict ourselves to CEAS absorbance below 0.2, where the use of the single-exponential approximation is fairly accurate (see Fig. 3c). The same procedure could of course be employed to relate the measured absorbance to the absorption coefficient, α, rather than the single-pass absorbance.

CO_2 Spectra. To verify the cavity ringdown technique, an alternative method for cavity calibration was used employing an absorber with a known absorption cross-section and concentration, in this case 100% CO_2 gas. Its wealth of ro-vibrational structure in the NIR region makes it well suited as a calibration species for the wavelength region covered in this study. A steady flow of 100% CO_2 gas was passed through a 1.15 m long Perspex tube inserted in the cavity. Figure 4a shows the cavity transmission (I) of the SC when the cavity is filled with CO_2. The spectrum was recorded on the OSA and corresponds to an average of 20 scans. From 1530 nm to 1650 nm the resolution changed from 32 pm to 21 pm, respectively. The corresponding absorbance spectrum, obtained by fitting a baseline (I_0) to the transmission and applying Eq. 1, is displayed in Fig. 4b. Overall the theoretical and experimental spectra are seen to agree well for absorbance values less than 0.2. Due to the finite resolution effects, the stronger lines of the absorption bands from 1565 nm to 1625 nm cannot be employed for reflectivity calibration. Furthermore, the weak band at 1640 nm is outside the high reflectivity region of the cavity mirrors. The weak band from 1528 nm to 1548 nm is therefore employed to verify the calibration. Figure 5a displays the experimental absorbance spectrum of this band along with its corresponding theoretical spectrum. The theoretical spectrum is calculated from Eqs. 2 and 3, with the measured reflectivity value taken from the cavity ringdown measurement. Here, $A_{\text{SP,THEORY}}$ in Eq. 3 corresponds to the single-pass absorbance of 100% CO_2 in the 1.17 m long cavity and was calculated based on line parameters from the HITRAN 2004 database.[34] To allow for a direct comparison between the experimental and theoretical spectra, the theoretical spectrum was convolved with a Gaussian filter, the width of which corresponds to the resolution of the OSA. Good agreement can be seen between the theoretical and experimental data in the
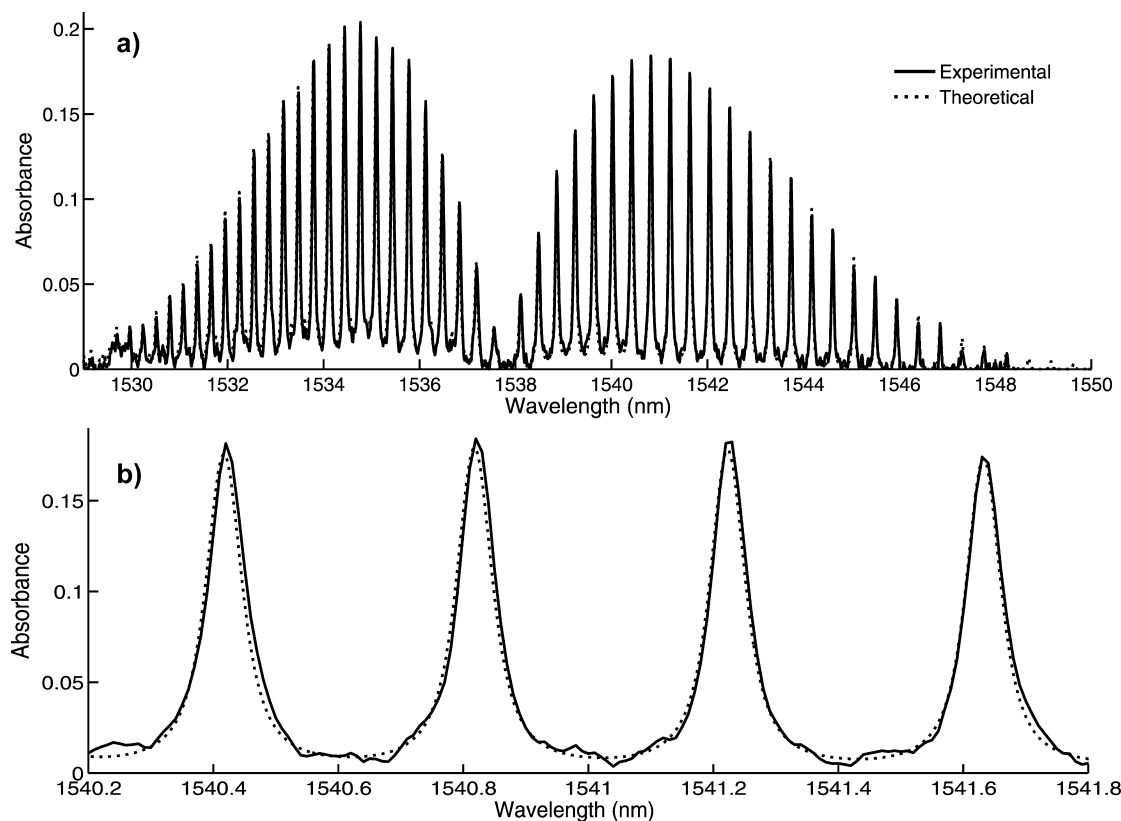
Fɪɢ. 5. (**a**) Measured absorption spectrum of the 30° ro-vibrational band of CO_2 (solid line), with the corresponding theoretical spectrum (dashed line) calculated using line parameters from the HITRAN database at experimental conditions ($L = 1.17$ m, $T = 297$ K, $p = 1001$ mbar, $X_{CO2} = 1.0$). (**b**) Magnified view of the 1540.2 nm to 1541.8 nm region showing a good match between experimental and HITRAN CO_2 peaks.

magnified view shown in Fig. 5b, indicating that the reflectivity value obtained using the cavity ringdown technique is reasonably accurate.

Similarly, a theoretical CO_2 spectrum generated in the same manner is displayed in Fig. 4c for the broader spectral range. The width of the Gaussian filter was varied across the spectral range to match the variation in the resolution of the OSA. The reflectivity across the spectral region was estimated by analyzing the weaker lines, which do not suffer finite resolution effects, and was found to vary from 97.4% at 1540 nm to 93.4% at 1640 nm. The reflectivity calculated from the gas calibration technique differs slightly from that obtained in the ringdown measurement. This is partly explained by the fact that the CO_2 band employed for calibration is centered around 1540 nm, whereas the ringdown calibration was centered around 1550 nm. For stronger lines a discrepancy is also observed due to finite resolution effects that are not fully compensated for. The baseline absorbance has a standard deviation of 3.1×10^{-3}, corresponding to a standard deviation in the absorption coefficient of 1.6×10^{-6} cm^{-1} at 1540 nm. With higher reflectivity mirrors the sensitivity could be improved. In our previous studies where we performed SC CEAS in the visible spectral range we were able to use mirrors with much higher reflectivity in conjunction with a more sensitive detector.[7] A ringdown time of 64 μs was achieved with mirrors of $R = 99.994\%$, in comparison to a ringdown time of 169 ns obtained in this work using mirrors having $R = 97.70\%$.

H₂O FLAME SPECTRA

In order to study high-temperature H_2O lines, a laminar flat flame burner was positioned in the center of the cavity. The premixed flame operates on a stoichiometric CH₄/air mixture at atmospheric pressure and has a diameter of 6 cm. The laser beam crossed the flame in the hot product zone, at a location 4 mm downstream of the flame front because the burner is specifically designed to achieve a homogeneous temperature distribution of around 2180 K at this height.[35] Probing close to the flame front itself is not advisable because the strong temperature gradients prevailing there were observed to cause severe beam steering in the cavity.

Figures 6a and 6b show the cavity absorbance structure observed with the flame off and the flame on, respectively. Here, 10 scans were averaged on the OSA at a resolution of 25 pm, resulting in an acquisition time of about half an hour. Weak absorption lines of H_2O at high temperatures can be observed between 1500 and 1550 nm. These high-temperature lines would be hard to observe in a direct absorption measurement but are clearly captured with the CEAS technique. A calculated spectrum corresponding to the experimental conditions and based on line strength and line shape data from the BT2 database[36] is shown in Fig. 6c. The overall structure of the spectra appears to agree well. Figure 6d shows a magnified view of the region between 1520 nm and 1523 nm. Although the overall structure is similar, there are discrepancies in exact line strengths and line positions, which are thought to be due to both database inaccuracies and limited signal-to-noise ratio of the experimental data. This access to
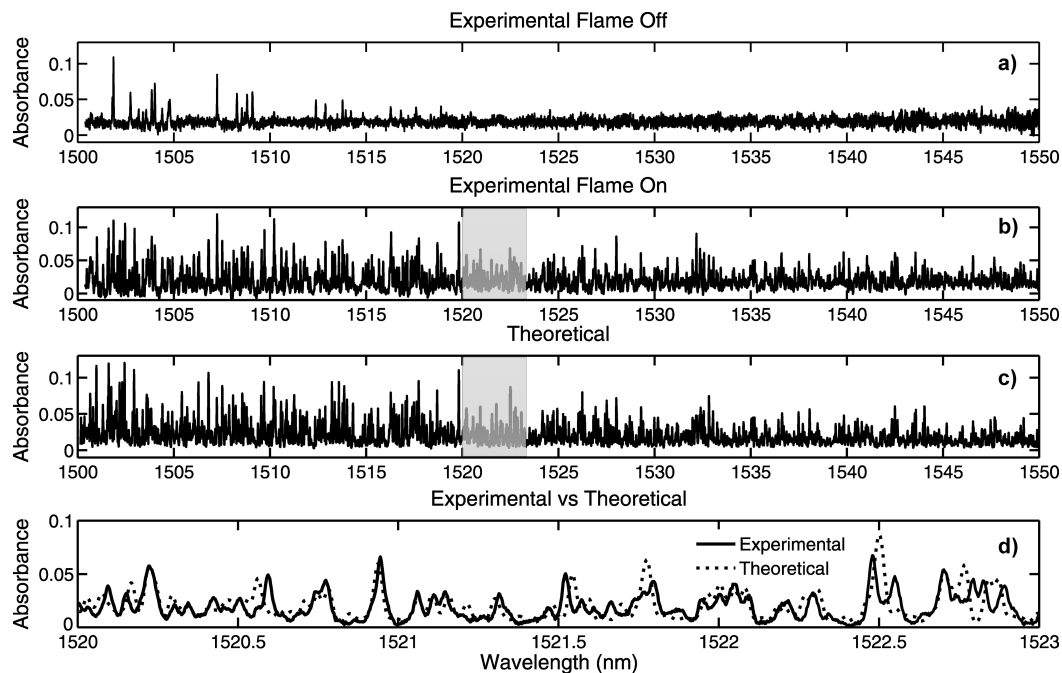
FIG. 6. (a) Experimental absorption spectrum, spanning from 1500 to 1550 nm, of cavity filled with ambient air. (b) Experimental absorption spectrum when a laminar flame was placed in the center of the cavity; the new lines appearing are all high-temperature H_2O lines. (c) Corresponding theoretical spectrum calculated using the line parameters from the BT2 database at experimental conditions ($L_{FLAME} = 60$ mm, $R = 0.974$, $T \sim 2180$ K (4 mm above burner), $p = 1001$ mbar, $X_{H2O} = 0.18$). The 1520 nm to 1523 nm region highlighted in grey is shown magnified in (d), where both experimental (b) and theoretical (c) H_2O peaks are plotted.

such broad spectral regions could allow for a more accurate validation of the theoretical databases, such as BT2[36] and HITRAN/HITEMP.[34]

STABILITY OF THE SETUP

In light of the long integration times employed using the OSA, it is of interest to study the stability of the CEAS setup. This can be quantified with the Allan deviation,[37] which is defined as

$$\sigma_y(\tau) = \sqrt{\frac{1}{M-1} \sum_{i=1}^{M} (y_{i+1} - y_i)^2} \qquad (4)$$
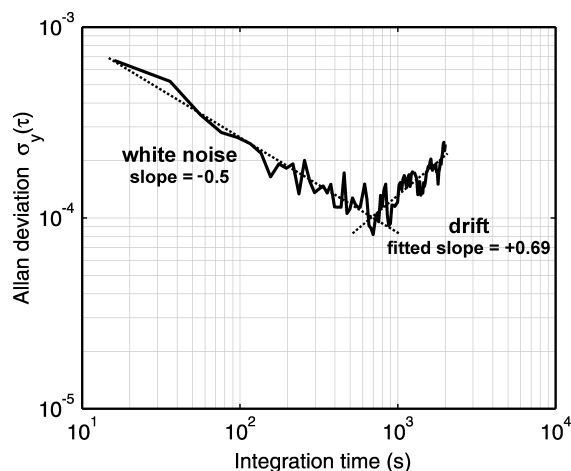

FIG. 7. Allan deviation of the transmitted intensity through an empty cavity at 1550 nm. The dotted lines are fits to the data.

where y_i is a set of M individual measurements of the intensity transmitted through the empty cavity, acquired at equally spaced time intervals. Here, the OSA scanned from 1500 nm to 1600 nm every 16 seconds at a resolution of 2 nm. Figure 7 plots the Allan deviation at 1550 nm. The Allan deviation of the transmitted intensity is characterized by white noise up to integration times of around 700 seconds. Beyond this point, drifts in the setup come into play. For optimum performance, the sample measurement and, if needed, the reference measurement must be accomplished within the white-noise-dominated period before any drifts take place.

CONCLUSION

A low-finesse broadband cavity enhanced absorption spectrometer, built around a supercontinuum excitation source, has been successfully employed for the study of high-temperature H_2O lines between 1500 nm and 1550 nm in a laminar flame. The experimental setup is straight forward, requiring only standard components found in many modern optical laboratories. The effective cavity reflectivity (97.7%) at 1550 nm was calibrated with a cavity ringdown technique, employing a fast photodetector to resolve the individual ringdown pulse profiles. CO_2 lines between 1520 nm and 1660 nm, acquired in pure CO_2 gas, were employed to validate the ringdown measurement, resulting in a reflectivity of $R = 97.4\%$ at around 1540 nm. For strong CO_2 lines finite resolution effects were observed, which could not be fully compensated for. Several improvements of the NIR super-continuum-based CEAS experiment presented here can be envisaged. With the broadband nature of the supercontinuum light source, the spectral bandwidth of the measurements could be extended, using either broader bandwidth mirrors or a prism cavity.[5] Detection limits could be improved by employing

higher finesse cavities, as was recently demonstrated in the visible spectral range,[7] whereas measurement speed could be substantially improved by employing a spectrometer fitted with an array detector rather than a scanning spectrum analyzer.[12] The simple experimental configuration and ease of generation of the SC radiation in the NIR potentially leads to applications in a number of combustion systems where water is a major product. Further work in low pressure flames could lead to the improvement of line parameters in the BT2 and HITRAN/HITEMP databases, therefore allowing more accurate experimental temperature determination in combustion systems.

ACKNOWLEDGMENTS

1. J. M. Dudley, G. Genty, and S. Coen, Rev. Mod. Phys. **78,** 1135 (2006).
2. A. R. Alfano, Ed., *The Supercontinuum Laser Source* (Springer, New York, 2006), 2nd ed.
3. C. F. Kaminski, R. S. Watt, A. D. Elder, J. H. Frank, and J. Hult, Appl. Phys. B: Lasers Opt. **92,** 367 (2008).
4. J. Hult, R. S. Watt, and C. F. Kaminski, J. Lightwave Technol. **25,** 820 (2007).
5. J. Hult, R. S. Watt, and C. F. Kaminski, Opt. Exp. **15,** 11385 (2007).
6. S. T. Sanders, Appl. Phys. B: Lasers Opt. **75,** 799 (2002).
7. J. M. Langridge, T. Laurila, R. S. Watt, R. L. Jones, C. F. Kaminski, and J. Hult, Opt. Exp. **16,** 10178 (2008).
8. P. Johnston and K. Lehmann, Opt. Exp. **16,** 15013 (2008).
9. M. Schnippering, P. R. Unwin, J. Hult, T. Laurila, C. F. Kaminski, J. M. Langridge, R. L. Jones, M. Mazurenka, and S. R. Mackenzie, Electrochem. Commun. **10,** 1827 (2008).
10. S. M. Ball, J. M. Langridge, and R. L. Jones, Chem. Phys. Lett. **398,** 68 (2004).
11. S. Vaughan, T. Gherman, A. A. Ruth, and J. Orphal, Phys. Chem. **10,** 4471 (2008).
12. M. J. Thorpe, D. Balslev-Clausen, M. S. Kirchner, and J. Ye, Opt. Exp. **16,** 2387 (2008).
13. G. Meijer, M. G. H. Boogaarts, R. T. Jongma, D. H. Parker, and A. M. Wodtke, Chem. Phys. Lett. **217,** 112 (1994).
14. J. Orphal and A. A. Ruth, Opt. Exp. **16,** 19232 (2008).
15. M. J. Thorpe and J. Ye, Appl. Phys. B: Lasers Opt. **91,** 397 (2008).
16. D. M. O'Leary, J. Orphal, A. A. Ruth, U. Heitmann, P. Chelin, and C. E. Fellows, J. Quant. Spectrosc. Radiat. Trans. **109,** 1004 (2008).
17. J. Mandon, G. Guelachvili, N. Picque, F. Druon, and P. Georges, Opt. Lett. **32,** 1677 (2007).
18. L. A. Kranendonk, A. W. Caswell, and S. T. Sanders, Appl. Opt. **46,** 4117 (2007).
19. R. S. Watt, C. F. Kaminski, and J. Hult, Appl. Phys. B: Lasers Opt. **90,** 47 (2008).
20. J. J. Scherer and D. J. Rakestraw, Chem. Phys. Lett. **265,** 169 (1997).
21. R. Peeters, G. Berden, and G. Meijer, Appl. Phys. B: Lasers Opt. **73,** 65 (2001).
22. J. Xie, B. A. Paldus, E. H. Wahl, J. Martin, T. G. Owano, C. H. Kruger, J. S. Harris, and R. N. Zare, Chem. Phys. Lett. **284,** 387 (1998).
23. S. Ball, J. Langridge, and R. Jones, Chem. Phys. Lett. **398,** 68 (2004).
24. J. M. Langridge, S. M. Ball, A. J. L. Shillings, and R. L. Jones, Rev. Sci. Instrum. **79,** 123110 (2008).
25. K. Stemaszczyk, M. Fechner, P. Rohwetter, M. Queißer, A. Czyżewski, T. Stacewicz, and L. Wöste, Appl. Phys. B: Lasers Opt. **3,** 369 (2009).
26. K. Stemaszczyk, P. Rohwetter, M. Fechner, M. Queißer, A. Czyżewski, T. Stacewicz, and L. Wöste, Opt. Exp. **17,** 3673 (2009).
27. M. Triki, P. Cermak, G. Méjean, and D. Romanini, Appl. Phys. B: Lasers Opt. **91,** 195 (2008).
28. S. M. Ball and R. L. Jones, Chem. Rev. **103,** 5239 (2003).
29. A. M. Shaw, R. N. Zare, C. V. Bennett, and B. H. Kolner, Chem. Phys. **2,** 118 (2001).
30. J. Martin, B. A. Paldus, P. Zalicki, E. H. Wahl, T. G. Owano, J. S. Harris, C. H. Kruger, and R.N. Zare, Chem. Phys. Lett. **258,** 63 (1996).
31. J. T. Hodges, J. P. Looney, and R. van Zee, J. Chem. Phys. **105,** 10278 (1996).
32. K. K. Lehmann and D. Romanini, J. Chem. Phys. **105,** 10263 (1996).
33. G. Herzberg, *Molecular Spectra and Molecular Structure: II. Infrared and Raman Spectra of Polyatomic Molecules* (D. Van Nostrand, New York, 1962), Chap. III, p. 274.
34. L. S. Rothman, D. Jacquemart, A. Barbe, D. C. Benner, M. Birk, L. R. Brown, M. R. Carleer, C. Chackerian, Jr., K. Chance, V. Dana, V. M. Devi, J.-M. Flaud, R. R. Gamache, A. Goldman, J.-M. Hartmann, K. W. Jucks, A. G. Maki, J.-Y. Mandin, S. T. Massie, J. Orphal, A. Perrin, C. P. Rinsland, M. A. H. Smith, J. Tennyson, R. N. Tolchenov, R. A. Toth, J. Vander Auwera, P. Varanasi, and G. Wagner, J. Quant. Spectrosc. Radiat. Trans. **96,** 139 (2005).
35. G. Hartung, J. Hult, and C. F. Kaminski, Meas. Sci. Technol. **17,** 2485 (2006).
36. R. J. Barber, J. Tennyson, G. J. Harris, and R. N. Tolchenov, Monthly Notices Roy. Astron. Soc. **368,** 1087 (2006).
37. P. Werle, R. Mücke, and F. Slemr, Appl. Phys. B: Lasers Opt. **57,** 131 (1993).